Applied Surface Science xxx (2018) xxx–xxx

Contents lists available at ScienceDirect

Applied Surface Science

journal homepage: www.elsevier.com/locate/apsusc

Full Length Article

Structural and magnetic properties of near surface superparamagnetic $Ni_{1-x}Fe_x$ nanoparticles in SiO_2 formed by low energy dual ion implantation with different fluences

Grant V.M. Williams[a,*], John Kennedy[b], Peter P. Murmu[b], Sergy Rubanov[c]

[a] The MacDiarmid Institute for Advanced Materials and Nanotechnology, SCPS, Victoria University of Wellington, PO Box 600, Wellington 6140, New Zealand
[b] National Isotope Centre, GNS Science, PO Box 31312, Lower Hutt 5010, New Zealand
[c] Advanced Microscopy Facility, Bio21 Institute, University of Melbourne, Victoria, 3010, Australia

ARTICLE INFO

Article history:
Received 15 October 2017
Received in revised form 19 January 2018
Accepted 29 January 2018
Available online xxx

Keywords:
$Ni_{1-x}Fe_x$
Ion implantation
Nanoparticles
Superparamagnetic
Magnetization

ABSTRACT

Low energy implantation of Ni and Fe into SiO_2 films resulted in the formation of superparamagnetic $Ni_{1-x}Fe_x$ nanoparticles for Ni fluences of 2×10^{16} at./cm^2, 4×10^{16} at./cm^2, and 6×10^{16} at./cm^2 where the Ni:Fe fluence ratios were 47:56, 53:47, and 63:37, respectively. Small ~5 nm $Ni_{1-x}Fe_x$ nanoparticles were dispersed in the implantation region for the lowest Ni fluence. Increasing the Ni fluence resulted in a different nanoparticle morphology where larger nanoparticles appeared at the surface and small $Ni_{1-x}Fe_x$ segregated regions to a depth of ~20 nm. The average nanoparticle size in the surface region was ~8 nm for Ni fluences of 4×10^{16} at./cm^2 and 6×10^{16} at./cm^2. The highest Ni fluence film also had smaller $Ni_{1-x}Fe_x$ nanoparticles at a depth of ~11 nm. The largest high field moment per implanted ion was found for the intermediate Ni fluence. The spin-stiffness was similar for all fluences and smaller than that expected for bulk $Ni_{1-x}Fe_x$. A small spin-disordered region was evident with the same low spin-freezing temperatures that may be due to a similar spin-disordered shells. dM/dH at 300 K was estimated and found to be highest for a Ni fluence of 4×10^{16} at./cm^2 where it reached 62.

1. Introduction

There is intensive ongoing research into magnetic nanoparticles because of their technological applications that include ultra-high density magnetic storage [1] and radio frequency components [2]. The small size of the magnetic nanoparticles can also potentially lead to new devices especially when they have a degree of electronic spin polarization and hence can display spin-dependent tunnelling [3–6], which is useful for ultra-small magnetic sensors and spin-transport magnetic RAM. The physics of nanoparticles can also be different from the bulk [7]. For example, they can have an enhanced magnetocrystalline anisotropy [7,8] as well as a different magnon dispersion for example via limiting of long wavelength magnon modes [9–11]. When magnetic nanoparticles are small enough they can also show superparamagnetic behaviour where there is minimal magnetic hysteresis [7,11]. This can be particularly useful for ultra-sensitive magnetic sensors where the size of the coercive magnetic field in bulk materials can limit the minimum detectable magnetic field. Magnetic nanoparticles have been made using a range of methods and small nanoparticles can have deleterious magnetic properties that include a reduced saturation magnetic moment and a low susceptibility [8,10,13,14]. It is therefore important to study alternative ways to make magnetic nanocompounds.

We have recently shown that low energy ion implantation of magnetic ions into different materials is a method that can be used to create magnetic nanostructures [15–18]. This can lead to large magnetoresistances as found by implantation of Fe into SiO_2 followed by electron beam annealing [15] that potentially be used in high magnetic field sensors. Dual implantation of Ni and Fe at low energies into SiO_2 has been shown to lead to small magnetic nanoparticles in the implanted layer that are superparamagnetic [17,18]. In a preliminary report, we showed that the susceptibility can also be enhanced [19]. However, it is not known if the nanoparticle morphology is altered by high Ni fluences or how the magnetic properties change as the Ni fluence is increased. The formation of superparamagnetic $Ni_{1-x}Fe_x$ after implantation is particularly interesting. Bulk $Ni_{1-x}Fe_x$ is known to have a remarkable small magnetocrystalline anisotropy and relatively high saturation moment that leads to very high magnetic susceptibilities [12]. This is useful

* Corresponding author.
E-mail address: Grant.williams@vuw.ac.nz (G.V.M. Williams).

https://doi.org/10.1016/j.apsusc.2018.01.277
0169-4332/

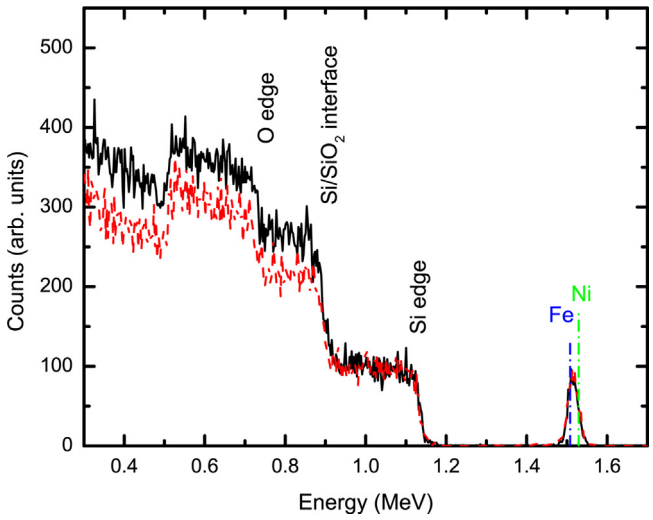

Fig. 1. RBS spectra for implanted SiO_2 films with Ni fluences of 4×10^{16} at./cm^2 (solid curve) and 6×10^{16} at./cm^2 (dashed curve) with the same Fe fluence of 3.5×10^{16} at./cm^2. The vertical lines shows the expected peak position for Fe and Ni.

for low field giant magnetoresistance (GMR) magnetic field sensors [20] and may be useful for flux-gate magnetometers [21].

In this paper, we report the results from dual implantation at low energies (10 keV) of Ni and Fe into SiO_2 films with Ni fluences of 4×10^{16} at./cm^2 and 6×10^{16} at./cm^2 and Fe fluence of 3.5×10^{16} at./cm^2. The results are compared with those from a previous report with a lower Ni fluence of 2×10^{16} at./cm^2 and a Fe fluence of 2.5×10^{16} at./cm^2 [17]. We show that the superparamagnetic $Ni_{1-x}Fe_x$ nanoparticles occur for all Ni fluences, the nanoparticle morphology is different for the Ni higher fluences, and the optimal magnetic properties occur for a Ni fluence of 4×10^{16} at./cm^2.

2. Materials and methods

The implantation of Ni and Fe into a 500 nm thick SiO_2 film on a 0.5 mm thick Si substrate was undertaken using the GNS Science implanter [22] at 10^{-7} mbar and with a current of <2 μA. The implantation energy was 10 keV and $^{58}Ni^+$ was implanted first and this was followed by $^{56}Fe^+$. Ni was implanted with a fluence, F_{Ni}, of 4×10^{16} at./cm^2 and Fe was implanted with a fluence, F_{Fe}, of 3.5×10^{16} at./cm^2 where $x = 0.47$. Another sample was made with a higher implanted Ni fluence of 6×10^{16} at./cm^2 and the same Fe fluence and hence $x = 0.37$. Rutherford backscattering spectroscopy (RBS) was performed at GNS Science with a He^+ beam energy of 2 MeV and a current of 10 nA [23] to measure the Ni and Fe concentrations in the SiO_2 film. Cross-sectional transmission electron microscope (TEM) measurements were made on samples that were first prepared using a focused ion beam lift-out method [24]. The samples were coated with carbon to reduce charging effects and then a Pt protection layer film was deposited. A FEI Tecnai TF 20 electron microscope operating at 200 kV was used for the TEM study. A Quantum Design magnetic measurements property system was used for the magnetic measurements where the applied magnetic field was parallel to the sample surface.

3. Results and discussion

The RBS spectra are plotted in Fig. 1 for Ni fluences of 4×10^{16} at./cm^2 and 6×10^{16} at./cm^2. The Si edge from Si in the SiO_2 layer can be seen at ~1.14 MeV and Si edge from the SiO_2/Si interface can be seen at ~0.89 MeV. The oxygen edge from oxygen in the SiO_2 layer is at ~0.74 MeV. The peak centred ~1.516 MeV is due to Ni and Fe in the implantation region. Separate Ni and Fe peaks cannot be resolved because of the RBS spectral resolution. They are expected to occur at 1.508 MeV and 1.529 MeV for Fe and Ni, respectively. The total Ni and Fe concentrations, c_T, in the SiO_2 films were obtained by fitting the RBS spectra using RUMP software [25]. They were 6.6×10^{16} at./cm^2 and 6.9×10^{16} at./cm^2 for Ni fluences of 4×10^{16} at./cm^2 and 6×10^{16} at./cm^2, respectively. The measured total Ni and Fe concentrations are 88% of the implanted fluences for the lowest Ni fluence and 73% of the implanted fluence for the highest Ni fluence. This reduction is due to sputtering of Ni during Ni implantation and Ni and Fe during Fe implantation. Dynamic TRansport of Ions into Matter (DTRIM [26]) simulations predict that c_T should be lower and it should be 3.7×10^{16} at./cm^2 where $x = 0.68$ for $F_{Ni} = 4 \times 10^{16}$ at./cm^2. c_T is predicted from DTRIM simulations to be 3.6×10^{16} at./cm^2 with $x = 0.67$ for the higher Ni fluence of $F_{Ni} = 6 \times 10^{16}$ at./cm^2. However, as shown below, nanoparticles formed during the implantation and hence the DTRIM cannot reliably predict the implanted ion fluences. Thus, the actual Ni and Fe concentrations are not known in the film although more Ni sputtering is expected for higher Ni fluences since Ni was implanted first.

Fig. 2a shows a TEM image from the implanted film with $F_{Ni} = 4 \times 10^{16}$ at./cm^2 where an implantation layer is evident and extending ~20 nm into the SiO_2 film. It apparent that $Ni_{1-x}Fe_x$ nanoparticles have formed during the implantation process and there is a nanoparticle layer close to the surface. The nanoparticle sizes were typically 7–10 nm although a smaller ~4 nm nanoparticle was also seen. The average nanoparticle diameter was ~8 nm. The rest of the implantation region contains very small $Ni_{1-x}Fe_x$ segregated regions. The effect of increasing the Ni fluence to 6×10^{16} at./cm^2 can be seen in Fig. 2b where a similar ~20 nm implantation region can be seen. The higher fluences still led to large $Ni_{1-x}Fe_x$ nanoparticles near the surface with sizes from 7 to 11 nm and an average diameter of ~8 nm. However, a smaller nanoparticle layer at a depth of ~11 nm is clearly evident further into the film where the nanoparticle sizes are ~3 nm. Small $Ni_{1-x}Fe_x$ segregated regions can be seen at larger depths.

The $Ni_{1-x}Fe_x$ nanoparticle morphology is completely different from than seen for a lower fluence. This is apparent in Fig. 2c where a TEM image is shown for $F_{Ni} = 2 \times 10^{16}$ at./cm^2 and $x = 0.56$ [17]. The lower fluence resulted in smaller nanoparticles extending over the entire implantation depth of ~24 nm where the average nanoparticles size was ~5 nm. The average nanoparticle sizes for all fluences are listed in Table 1.

The different nanoparticle sizes and depth distributions seen for low and higher Ni fluences is likely to be due to a higher Ni fluence in the surface region, implanted ion sputtering, and diffusion during implantation. Higher Ni fluences led to an increase in the nanoparticle size in the surface nanoparticle layer that appears to saturate at and above $F_{Ni} = 4 \times 10^{16}$ at./cm^2.

Magnetic measurements were undertaken and the magnetic moment per implanted ion, m_{ion}, is plotted against the magnetic field, B, in Fig. 3a for $F_{Ni} = 4 \times 10^{16}$ at./cm^2 and in Fig. 3b for $F_{Ni} = 6 \times 10^{16}$ at./cm^2. m_{ion} was obtained using

$$m_{ion} = [m - \chi_{Si} \times V \times B/\mu_0]/[[c_{Ni} + c_{Fe}] \times A], \quad (1)$$

where m is the measured moment, χ_{Si} is the silicon substrate susceptibility, V is the sample volume, μ_0 is the permittivity of free space, c_{Ni} is the Ni concentration in at./cm^2, c_{Fe} is the Fe concentration in at./cm^2, and A is the sample area. The appearance of a large m_{ion} at high B is indicative of ferromagnetic order from $Ni_{1-x}Fe_x$ nanoparticles and the data in Fig. 3 shows that the Curie temperature is above 300 K. Bulk $Ni_{1-x}Fe_x$ has Curie temperatures that depend on the Fe fraction and ranges between 473 K–1144 K [27].

Please cite this article in press as: G.V.M. Williams, et al., Structural and magnetic properties of near surface superparamagnetic $Ni_{1-x}Fe_x$ nanoparticles in SiO_2 formed by low energy dual ion implantation with different fluences, Appl. Surf. Sci. (2018), https://doi.org/10.1016/j.apsusc.2018.01.277